

Communications

Detection of Tunnels in Low Loss Media Illuminated by a Transient Pulse

John Schneider and Irene C. Peden

Abstract—The field scattered from a subsurface object illuminated by a transient pulse is determined using the T -matrix method. Although the method itself is a resonance-region, frequency-domain technique, it is shown that it can be applied to problems in which the pulse has energy that spans several decades in the frequency domain. The illuminating pulse simulates one used in an actual VHF subsurface radar exploration device. The pulse is radiated from an electric dipole in a vertical borehole.

The scattered pulse is obtained by first calculating the components in the spectral description of the transmitting antenna current. The T -matrix method is then used to determine the system transfer function, which, in turn, gives the scattered energy in terms of the antenna current. An inverse Fourier transform yields the temporal scattered field. The scatterer is modeled as a dielectric ellipsoid, which is presented as an approximation to a cylindrical tunnel. Results are compared to those obtained from a field experiment in which a deeply buried tunnel embedded in granite was illuminated by a dipole source.

I. INTRODUCTION

Recently there has been much interest in subsurface exploration at sites where boreholes are present [1]–[4]. Cross-borehole probing has been used successfully at such sites to locate tunnels surrounded by hard rock (e.g., [5]). In an earlier paper [6], a theoretical technique was presented for studying subsurface scattering utilizing the T -matrix method, an approach more general than earlier techniques proposed to study the cross-borehole scattering problem. It permits an arbitrary orientation of the source relative to the scatterer and an electric dipole formulation for the source; the scatterer is approximated as an ellipsoid. The air-ground interface is assumed to be sufficiently distant from the target that its effects can be neglected. However, the results presented in [6] are limited to continuous wave illumination whereas field experiments often employ transient signals. Since the T -matrix method is inherently a resonance-region, frequency-domain technique, it was not entirely clear at the outset that this approach could be used to study subsurface scattering under transient illumination. This paper demonstrates its suitability for examination of a typical subsurface scattering problem. The illuminating pulse used approximates that of the Pulsed Electromagnetic Search System (PEMSS) developed at Southwest Research Institute [7]. Some success has been reported with the use of this system in the detection of tunnels [7]–[10].

Accurate modeling of scatter from a tunnel is the objective. The tunnel dimensions and the constitutive parameters of the host medium considered here are based on those measured at an actual site.¹ The tunnel is assumed to be between boreholes that are 20 m apart. The

transmitting and receiving antennas are lowered simultaneously to obtain a borehole logging.

The T -matrix method, as used in [6], requires that the scatterer be of finite extent. Therefore, the tunnel is modeled as an ellipsoid. By using an elongated spheroid or ellipsoid as a model, the cross section of the tunnel is well approximated in the area closest to the illuminating source. The tunnels of interest to this study have cross sections that are straight on three sides with a domed top. In Section III, the ellipsoidal scatterer has a total axial dimension of 6.6 m, a height of 2.2 m, and a width of 1.8 m. These cross-sectional dimensions closely approximate those of the pertinent tunnels while the axial dimension was chosen long enough to provide a realistic approximation to a segment of the tunnel but not so long as to cause problems with the condition number of the matrices.

Steps needed to employ the previously reported T -matrix approach to the transient subsurface scattering problem are outlined in Section II. In Section III, results are presented. Concluding remarks are given in Section IV.

II. TIME DOMAIN APPROACH

Due to practical limitations the T -matrix method cannot be used in problems in which the wavelength is much less than a typical dimension of the scatterer. However, by using Fourier transforms, the method can be used to study a time domain scattering problem in which the illuminating pulse in the frequency domain spans several decades but the bulk of its energy is in the resonance region. This section outlines the necessary steps to accomplish this. The reader is directed to [6] and [11]–[14] for details of the T -matrix method.

A transient pulse of current, assumed to exist on an infinitesimally small vertical electric dipole, gives rise to a radiated field. A T -matrix is found for each harmonic of this pulse to determine how energy is scattered at that frequency. This yields a spectral description of the scattered field which is inverse Fourier transformed to obtain the desired temporal scattered pulse.

The PEMSS pulse can be closely approximated by assuming the antenna current is a 40 MHz sinusoid that is weighted by a Gaussian envelope and passed through a low Q bandpass filter. The weighted sinusoidal signal $i(t)$ is given by

$$i(t) = \begin{cases} 0 & \text{if } t < 0 \\ \sin(\omega_c t) e^{-(t-d)^2/\tau^2} & \text{otherwise} \end{cases} \quad (1)$$

where $d = 12\Delta$ is an offset, $\omega_c = 2\pi \cdot 40 \times 10^6$ rad/s, and $\tau = 1.25 \mu\text{s}$ is a time constant. The time $\Delta = 1.953125$ ns is the interval used for sample spacing in the time domain and was chosen for convenience for performing the Fourier transforms. This sampling interval in the time domain corresponds to a sampling interval of 2 MHz in the frequency domain. The Fourier transform of $i(t)$ is $I(\omega)$. The transfer function for the bandpass filter is

$$B(\omega) = \frac{\omega_0^2}{-\omega^2 - i\omega\omega_0/1.2 + \omega_0^2} \quad (2)$$

where $\omega_0 = 2\pi \cdot 20 \times 10^6$ rad/s. The product $I(\omega)B(\omega)$ is the frequency domain representation of the current on the transmitting dipole antenna. This is a purely heuristic description of the antenna current, but it shows good agreement with the observed radiated pulse. The function $I(\omega)$ was obtained by taking a 256-point FFT of $i(t)$

Manuscript received February 7, 1992; revised August 21, 1992.

J. Schneider is with the School of Electrical Engineering and Computer Science, Washington State University, Pullman, WA 99164-2752.

I. C. Peden is with the Department of Electrical Engineering, University of Washington, Seattle, WA 98195. She is presently on leave at the National Science Foundation, Division of Electrical and Communication Systems, Room 1151, 1800 G Street, NW, Washington, DC 20550.

IEEE Log Number 9206401.

¹Courtesy of the U.S. Army.

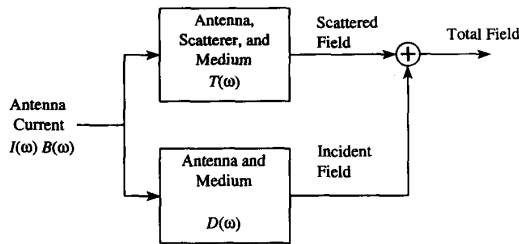


Fig. 1. Block diagram of the scattering system.

with a sample spacing of Δ . The greatest contribution to $I(\omega)B(\omega)$ occurs at approximately 22 MHz, with the power at 2 MHz and 62 MHz approximately 20 dB down from that at 22 MHz.

The function $I(\omega)B(\omega)$ gives the magnitude and phase of each spectral component of the antenna current. When multiplied by the appropriate T -matrix, a spectral description of the scattered field is obtained. The T -matrix is essentially the transfer function for the transmitting antenna, the host medium, and the scatterer. Alternatively, when multiplied by the transfer function of a dipole, the spectral components of the radiated, or incident, pulse are obtained. A block diagram of the system is given in Fig. 1. The transfer function obtained from the T -matrix method is labeled $T(\omega)$ and the dipole transfer function is labeled $D(\omega)$.

The dipole antenna is vertical, with θ defined as the angle from its longitudinal axis to the observation point. The θ component of the radiated field is oriented in the direction of increasing θ . The θ component of the radiated pulse is obtained by multiplying the spectral description of the antenna current by the θ component of the dipole transfer function given by

$$D_{\theta}(\omega) = -i\omega\mu \frac{1}{4\pi r} \left(1 - \frac{1}{\gamma r} + \frac{1}{\gamma^2 r^2} \right) \sin(\theta) e^{\gamma r} \quad (3)$$

where $\gamma = ik = i\omega\sqrt{\epsilon\mu}$ is the propagation constant. $D_{\theta}(\omega)$ is also a function of the distance r from the dipole and of the medium constitutive parameters. Because the transmitter and receiver are lowered simultaneously, maintaining the same depth, the receiver is always at an angle of $\theta = 90^\circ$ relative to the transmitter. Thus, the θ component of the field corresponds to the negative of the vertical component. This is the only component measured by the vertical receiver. The vertical component of the radiated pulse is shown in Fig. 2 when the observation point is 8 m, 12 m, 16 m, and 20 m from the dipole and the medium has a conductivity $\sigma = 0.002$ S/m, a relative permittivity $\epsilon_r = 9.00$, and a relative permeability $\mu_r = 1.00$; these constitutive parameters are approximately those of granite at VHF frequencies. The radiated pulse is seen to have a duration slightly greater than $0.1 \mu\text{s}$ and to decay rapidly with distance from the source. This is due to both the $1/r$ behavior of dipole radiators and to the exponential decay imparted by loss in the medium. The exponential decay is given by $e^{\text{Re}(\gamma r)}$ and is frequency dependent. Using 22 MHz, which is the most energetic frequency of antenna current in this example, and the constitutive parameters given above, the rate of decay is $e^{-0.12508r}$. Thus, at 22 MHz the field decays an amount $1/e$ approximately every 8 m due to loss in the medium. Fig. 3 presents the same information in spectral, rather than temporal, form. Fig. 3 shows that the propagation of the pulse has little effect on the distribution of energy in the harmonics, i.e., the magnitude is uniformly affected. This is as expected since $e^{\text{Re}(\gamma r)}$ changes little with frequencies above 10 MHz.

The matrices used to determine the scattered field become more poorly conditioned as the frequency is increased. A frequency exists beyond which the results of the T -matrix method are not accurate,

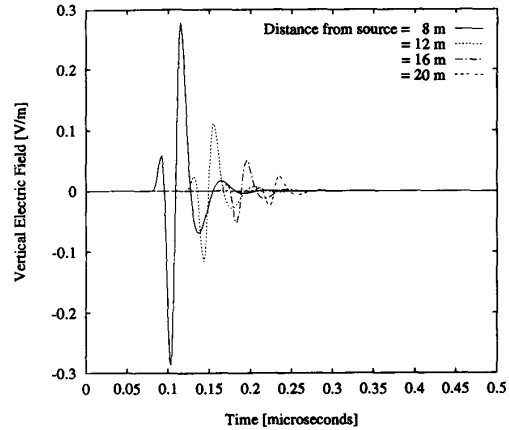


Fig. 2. Vertical component of the radiated pulse as a function of time at points 8 m, 12 m, 16 m, and 20 m from the dipole.

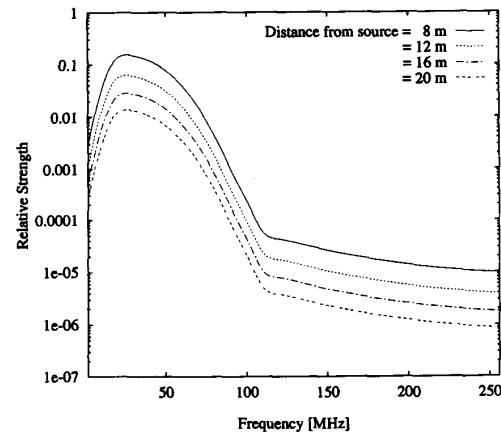


Fig. 3. Spectral components of the radiated pulse as a function of frequency at points 8 m, 12 m, 16 m, and 20 m from the dipole.

and frequencies above this point cannot be used. This limitation is imposed by practical considerations such as finite numeric precision and finite memory. The limitation of the T -matrix method is equivalent to bandlimiting the scattered pulse. The size of the scatterer and the constitutive parameters dictate that scattered energy above 72 MHz cannot be considered for the results given in Section III since the T -matrix beyond 72 MHz cannot be calculated reliably. A radiated pulse that is bandlimited to 72 MHz and measured 8 m from the transmitter is shown in the frequency domain in Fig. 4 and in the time domain in Fig. 5. Even though the spectral representations of the truncated and untruncated pulses are quite dissimilar, the temporal representations are similar since the majority of the energy is below the cut-off frequency of 72 MHz. An artifact of truncation is that the pulse in Fig. 5 has some "ringing" not present in the untruncated pulse. In Section III, the radiated pulse is not bandlimited. However, the scattered pulse is bandlimited since the T -matrix was used to obtain it. The radiated pulse with frequency truncation in Figs. 4 and 5 illustrates the effects of bandlimitation on the synthesis of a pulse. Any persistent or anticausal fluctuations seen in the scattered pulse are the effect of a limited number of harmonics rather than an indication of a scatterer resonance, such as creeping waves, or an underlying error in the approach.

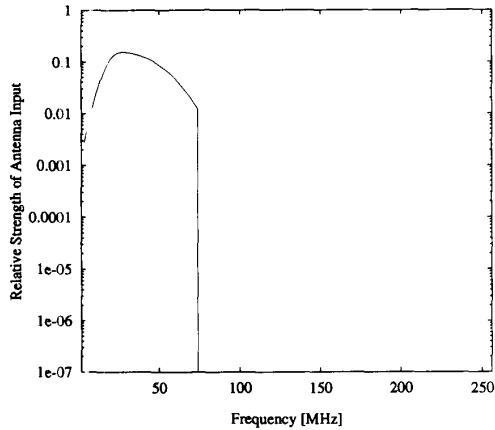


Fig. 4. Magnitude of the spectrum of the radiated pulse when the contribution from frequencies above 72 MHz is set to zero.

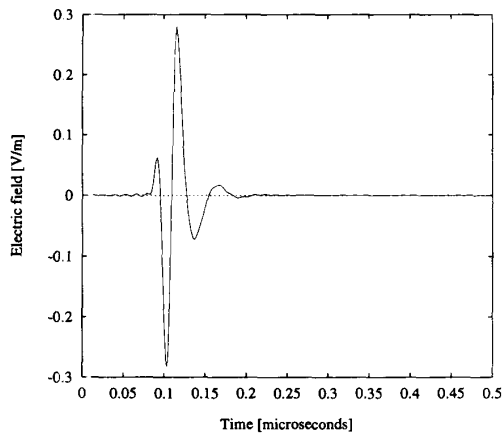


Fig. 5. The radiated pulse when the contribution from frequencies above 72 MHz is set to zero.

To use the T -matrix method as previously formulated [6], the magnitude and phase of the antenna current must be multiplied by $-k^2 \eta \frac{1}{\sqrt{6\pi}}$, where $\eta = \sqrt{\mu/\epsilon}$ and $k = \omega\sqrt{\mu\epsilon}$. Thus, given the antenna current $I(\omega)B(\omega)$ weighted by $-k^2 \eta \frac{1}{\sqrt{6\pi}}$, the scattered field can be obtained. To obtain the total field, the incident pulse can be added to the scattered field.

III. RESULTS

Fig. 6 shows two perspectives of the vertical component of the scattered pulse measured in the receiver borehole as a function of time and elevation calculated using parameters and dimensions identified in the previous sections. A 256-point Fourier transform was used and the ellipsoid was horizontally centered between boreholes that were 20 m apart. Elevations are relative to the center of the scatterer; thus, zero elevation occurs when the antennas are at the same depth as the center of the scatterer. The field was calculated over a 20 m segment of the borehole. The calculation shown in the figure starts when $t = 0.16 \mu\text{s}$ and ends when $t = 0.32 \mu\text{s}$. Time is measured relative to $t = 0$ in (1). The scattered electric field is plotted using a linear scale. Numeric noise, seen as ringing before and after the arrival of the pulse, is visible in this figure. The arrival time increases and

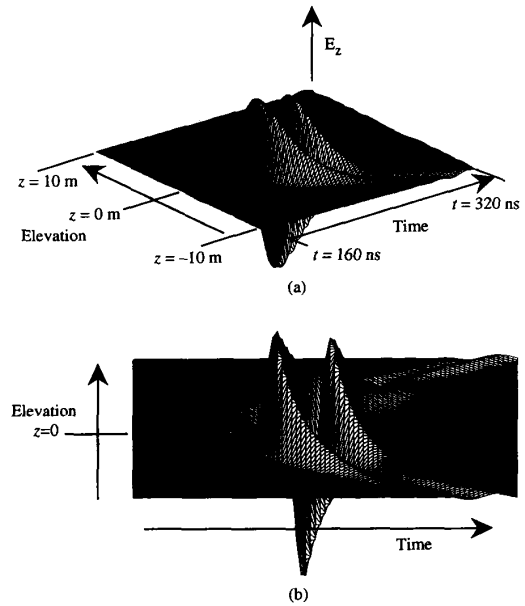


Fig. 6. Pulse scattered from an ellipsoid measured in a 20 m segment of the borehole containing the receiver when the distance between boreholes is 20 m. (a) Rotated view. (b) View looking perpendicular to time axis.

magnitude of the pulse decreases with decreased proximity to the scatterer.

The decrease in the scattered field with decreased proximity is partly due to increased path length and, hence, increased loss. Other factors contribute to this decrease and these factors would be present even in a lossless medium. One of these factors is the finite size of the ellipsoidal scatterer. As the transmitting antenna is moved away from the scatterer, the finite scatterer presents a smaller target to the radiated pulse. Another factor is the orientation of the receiving dipole antenna. In the assumed geometry, the receiver only measures the vertical component of the scattered field, i.e., the fields along the borehole axis. As the receiver is moved away from the scatterer, the vertical component of the scattered field decreases while the horizontal component increases.

The direct field has been added to the scattered field in Fig. 7. Since the transmitter and receiver are assumed to be at the same elevation, the direct field does not vary as the elevation is changed. Therefore, the total field is quickly dominated by the direct field as the proximity of the scatterer is decreased. Points of constructive and destructive interference are evident in Fig. 7. The constructive interference occurs in the vicinity of zero elevation, whereas the destructive interference is present at approximately ± 3 m of elevation. In Fig. 7(b) the scattered field is visible as a small ripple that arrives after the direct field for elevations away from zero. The pattern is similar to a hyperbola and serves as an important diagnostic of scatterer location [9], [15]. In the vicinity of zero elevation, some energy arrives prior to the incident pulse. This is due to the faster speed of propagation through the air-filled tunnel and serves as another diagnostic of scatterer location and tunnel contents.

The results shown in Figs. 6 and 7 can be compared to the field data obtained from PEMSS² that is shown in Fig. 8. These results pertain to a deeply buried tunnel that has a typical cross-sectional dimension of 2 m and is surrounded by granite. The borehole spacing is 20 m.

²Data obtained from the PEMSS II VHF Subsurface Radar developed at Southwest Research Institute.

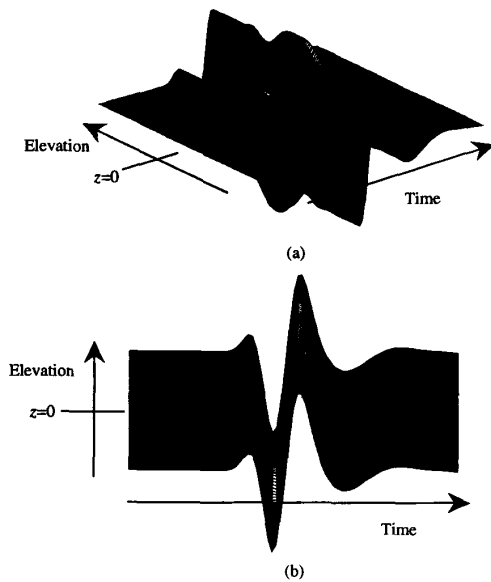


Fig. 7. Sum of direct pulse and pulse scattered from an ellipsoid measured in a 20 m segment of the borehole containing the receiver when the distance between boreholes is 20 m. (a) Rotated view. (b) View looking perpendicular to time axis.

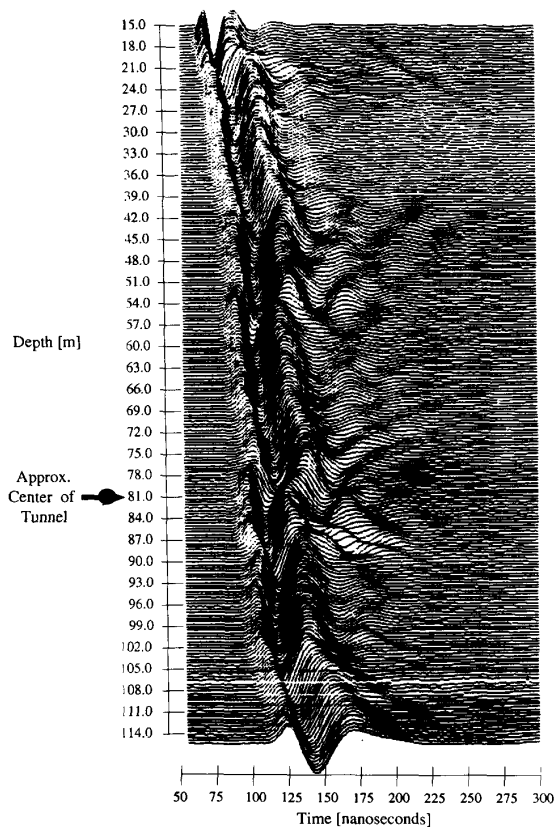


Fig. 8. PEMSS results for 20 m borehole separation.

The approximate location of the tunnel is indicated on the vertical axis. The PEMSS results clearly show the "hyperbolic wings" that are evident in Figs. 6 and 7, and the earlier arrival of the leading edge of the pulse in the tunnel vicinity where energy has passed through the tunnel.

The time needed to calculate the scattered field was dominated by the calculation of the 36 T -matrices. The length of each of these calculations was a function of the number of elements in the matrix and that was dictated by the frequency. The size of the matrices ranged from a low of 126×126 at 2 MHz to high of 390×390 at 72 MHz, corresponding to CPU times of 1 to 14 min on an IBM RS6000.

IV. SUMMARY

The fields scattered by a subsurface ellipsoid under pulsed illumination can be determined using the T -matrix and Fourier transform methods. This approach is restricted to cases in which the energy in the illuminating pulse lies predominately in the resonance region of the scatterer.

Scattering from a tunnel that is illuminated using the PEMSS system is well suited to investigation using the method described here. The results from this method show both the hyperbolic wings that serve as an important diagnostic of scatterer location and the expected earlier arrival time of pulses that have traveled through the air-filled tunnel. This approach also can be used to investigate the fields scattered under any arbitrary rotation of the scatterer relative to the transmitter and receiver [6].

REFERENCES

- [1] P. Maass, "S. Korean U.S. Officials find tunnel from North," *Washington Post*, Mar. 4, 1990.
- [2] Belvoir Equipment Finds DMZ Tunnel, *Pentagram*, Mar. 15, 1990.
- [3] J. Clausen, "EM-field technology helps locate tunnels, abandoned mines," *Sandia National Laboratories*, vol. 43, no. 11, 1991.
- [4] M. Sato and R. Thierback, "Analysis of a borehole radar in cross-hole mode," *IEEE Trans. Geosci. Remote Sensing*, vol. 29, pp. 899-904, 1991.
- [5] R. J. Lytle, E. F. Laine, D. L. Lager, and D. T. Davis, "Cross-borehole electromagnetic probing to locate high-contrast anomalies," *Geophysics*, vol. 44, no. 10, pp. 1667-1676, 1979.
- [6] J. Schneider, J. Brew, and I. Peden, "Electromagnetic detection of buried dielectric targets," *IEEE Trans. Geosci. Remote Sensing*, vol. 29, pp. 555-562, 1991.
- [7] T. E. Owen and S. A. Shuler, "Subsurface void detection using surface resistivity and borehole electromagnetic techniques," in *Tech. Prog. Abstracts and Biographies, 50th Annual International Meeting and Exposition* (Houston, TX), Society of Exploration Geophysicists, 1980.
- [8] G. R. Olhoeft, "Interpretation of hole-to-hole radar measurements," in *Proc. of Third Tech. Symp. on Tunnel Detection* (Golden, CO), Jan. 1988.
- [9] R. Greenfield, "Modeling of electromagnetic propagation between boreholes," in *Proc. of Third Tech. Symp. on Tunnel Detection* (Golden, CO), Jan. 1988.
- [10] R. Greenfield, "Electromagnetic, frequency domain modeling of tunnel signature," Department of the Army, U.S. Army Ballistic Research Laboratory, Aberdeen Proving Ground, MD, GL-90-1, Sept. 1990.
- [11] P. C. Waterman, "Matrix formulation of electromagnetic scattering," *Proc. IEEE*, vol. 53, pp. 805-812, 1965.
- [12] P. C. Waterman, "Symmetry, unitarity, and geometry in electromagnetic scattering," *Phys. Rev. D*, vol. 3, no. 4, pp. 825-839, 1971.
- [13] P. Barber and C. Yeh, "Scattering of electromagnetic waves by arbitrary shaped dielectric bodies," *Appl. Opt.*, vol. 14, no. 12, pp. 2864-2872, 1975.
- [14] J. B. Schneider and I. C. Peden, "Differential cross section of a dielectric ellipsoid by the T -matrix, extended boundary condition method," *IEEE Antennas Propagat.*, vol. 36, no. 9, pp. 1317-1321, 1988.
- [15] R. C. Kemeraik, J. N. Griffin, J. L. Meade, G. D. Kraft, and G. W. Pound, "Signal processing applied to tunnel detection by borehole radar," in *Proc. of Third Tech. Symp. on Tunnel Detection* (Golden, CO), Jan. 1988.